Supporting Information:

3D Printed Quantum Dot Light-Emitting Diodes

Yong Lin Kong[†], *Ian A. Tamargo*[§], *Hyoungsoo Kim*[†], *Blake N. Johnson*[†], *Maneesh K. Gupta*[†], *Tae-Wook Koh*[‡], *Huai-An Chin*[‡], *Daniel A. Steingart*[†#], *Barry P. Rand*[‡#], *Michael C. McAlpine*[†]*

[†]Department of Mechanical and Aerospace Engineering, Princeton University, Princeton, NJ 08544.

[§] Department of Chemistry, Princeton University, Princeton, NJ 08544.

[‡]Department of Electrical Engineering, Princeton University, Princeton, NJ 08544.

[#]Andlinger Center for Energy and the Environment, Princeton University, Princeton, NJ 08544

*Corresponding author, Telephone number: (609) 542-0275, E-mail: mcm@princeton.edu

3D Printer

An industrial robotic dispenser (Fisnar, Wayne, NJ) was modified into a multi-head 3D printer, where up to four different inks can be loaded and independently controlled with an external I/O card and pressure regulators (Fig. S1). The printer supports standard size syringe barrels, and universal luer-lock needles. Tips from 27 to 33 gauge (GA) have been used depending on the material viscosity and resolution required. For high precision printing, the barrel pressure was regulated from 0 to 100 psi with a digital pressure regulator (Nordson Corporation, Westlake, OH). Vacuum suction control of the regulator was used to prevent dripping of low viscosity fluids. Higher viscosity inks were independently regulated with analog pressure regulators (Fisnar, Wayne, NJ) for multi-material printing. The distance registration was calibrated with a digital CMOS laser sensor (Keyence, Itasca, IL), and the printer stage has a maximum resolution of 1 μm per axis. Control of the 3D printer was achieved via custom-written LabVIEW programs through serial connection. Commercially available CAD software, Solidworks Premium 2014 (Dassault Systèmes, Vélizy-Villacoublay Cedex, France) was used for all modeling applications. The typical printing strategy involved the formatting of 3D CAD files into stereolithography (STL) format, followed by slicing the model into G-code coordinates. The G-code was then translated to the command language of the robotic dispenser via a custom-written LabVIEW program. In some instances, a Peltier stage heater was used and the temperature was modulated with the applied voltage to optimize the printing condition or for annealing the printed film. A UV laser (405 nm) was also integrated to the printer arm to provide curing of photoactive materials, such as the UV adhesive.

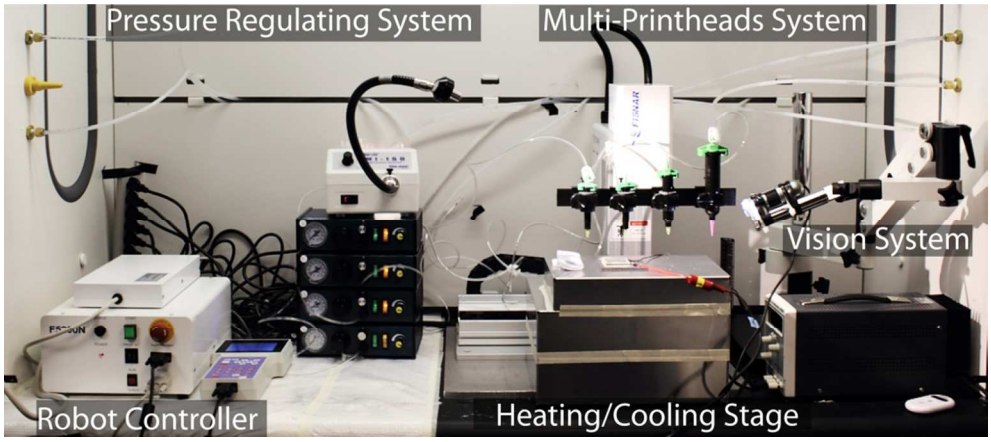

Figure S1. Multi-material 3D printer with its major components labelled.

3D Printed Quantum Dot Light Emitting Diodes (QD-LEDs)

A regular glass slide was cleaned with water, acetone and isopropanol for 15 minutes each. Circular rings of 1.5 mm radius connected to contact pads were then printed using a synthesized silver nanoparticle (AgNP) ink. The anode ring was printed with a 3 cc syringe barrel through 33 ga nozzles (108 µm inner diameter) with a barrel pressure of 20 psi (Fig S2A). The printer translation speed was maintained at 0.5 mm/s, and the distance between the nozzle tip and the substrate was kept at 85 µm. The printed silver was annealed at 200 ºC for 3 hours. PEDOT:PSS (Sigma Aldrich, St. Louis, MO) was then dispensed at the center of the ring until the contact line touched the ring. The substrate was then heated to 150 ºC for 15 minutes, which resulted in a transparent and conductive film. A 0.15 wt% poly-TPD (American Dye Source Inc, Quebec, Canada) solution in chlorobenzene was then dispensed and heated at 150 ºC for 30 minutes. Subsequently, a 1 mg/ml of CdSe/ZnS QD solution with either green (Ocean NanoTech, San Diego, CA) or orange-red (Ocean NanoTech, San Diego, CA) in a co-solvent mixture was then dispensed onto the annealed poly-TPD. The printed QD droplet was allowed to evaporate completely without heating in a petri dish. Note that for printing of PEDOT:PSS, poly-

TPD and QDs, the ink was loaded into a 3 cc syringe barrel with a 32 ga nozzle. The nozzle was registered to position at the center of anode ring. Ink was prevented from dripping by applying a vacuum with a digital pressure regulator. During printing, the vacuum was turned off, the nozzle was lowered until the ink at the tip of the nozzle touched the substrate, and the position was held. The amount of ink extruded was controlled by controlling the hold-time (Fig. S2B), which corresponds to an extrusion of approximately 0.8 μL. After printing, the nozzle was raised and vacuum was resumed to prevent dripping of the ink. Upon complete drying of QDs, EGaIn (Sigma Aldrich, St. Louis, MO) was then printed at the center of the ring with a digital pressure regulator to form a conformal liquid metal cathode. The 33 ga nozzle with a 3 cc barrel loaded with EGaIn was lowered to a gap of 100 μm from the surface of printed QD. A pressure of 4.5 psi was then applied for 3 seconds to print a hemispherical liquid cathode to cover the quantum dots. UV adhesive (Novacentrix, Austin, TX) was then printed through 33 ga nozzle, at a 50 μm gap with the printed anode, with a 5 mm/s translation speed around EGaIn to insulate it from the AgNP anode ring. The printed adhesive was then cured with a 405 nm laser attached to the 3D printer (Fig. S2C). Conductive silicone (Silicone Solutions, Cuyahoga Falls, OH) was then printed in order to contact the exposed printed EGaIn with a pad before it was left overnight to vulcanize completely. UV adhesive (Novacentrix, Austin, TX) was printed using the aforementioned parameters and cured with the 405 nm laser to encapsulate the printed QD-LEDs. This process flow is illustrated in Fig. S3. The thicknesses of the individual layers was measured by profilometry to be the following: AgNP silver ring, 80 μm; PEDOT:PSS, 200-300 nm; poly-TPD, 100-200 nm; quantum dots, 100-150 nm; EGaIn, 2-3 mm. The QD-LED as fabricated was characterized with a source measure unit (Agilent, Santa Clara, CA), spectra were obtained with a spectrometer (Ocean Optics, Dunedin, FL), and the luminance was calibrated

with a luminance meter (Konica Minolta, Ramsey, NJ). All measurements were done under ambient conditions.

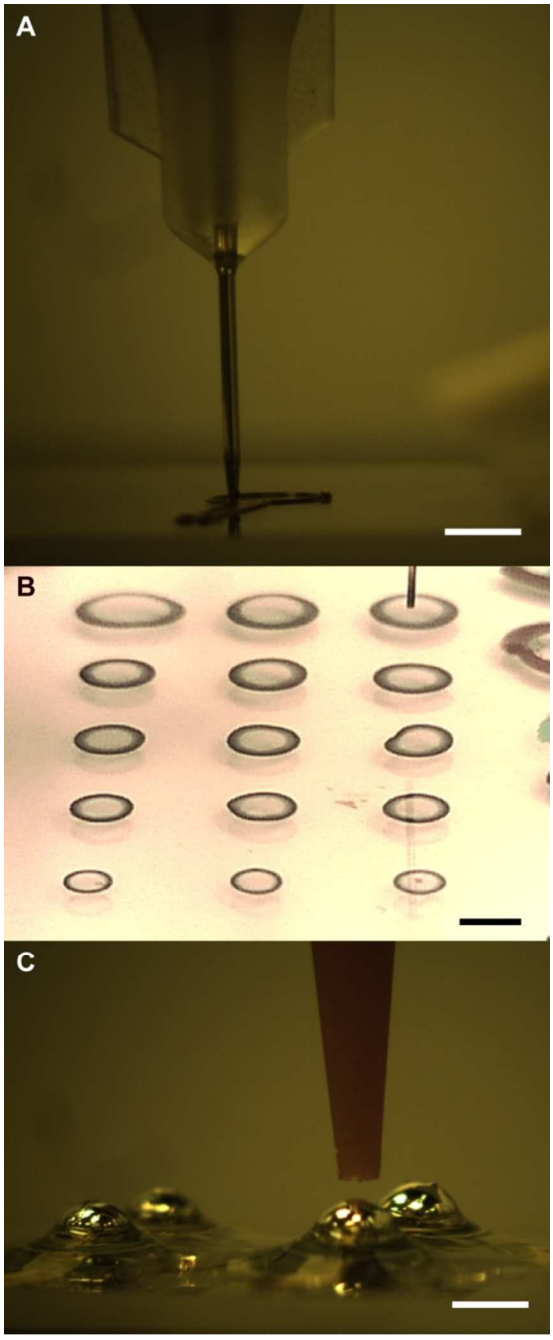

Figure S2. 3D printed QD-LED extrusion. **(A)** Printing of a silver anode ring. Scale bar is 5 mm. **(B)** Control of low viscosity ink deposition size with different nozzle hold-times. Increasing the hold time increases the printed dimension. Scale bar is 5 mm. **(C)** Fully 3D printed QD-LED, covered with insulating UV adhesive, with exposed EGaIn which would subsequently be connected with conductive RTV silicone to contact pads. Scale bar is 2 mm.

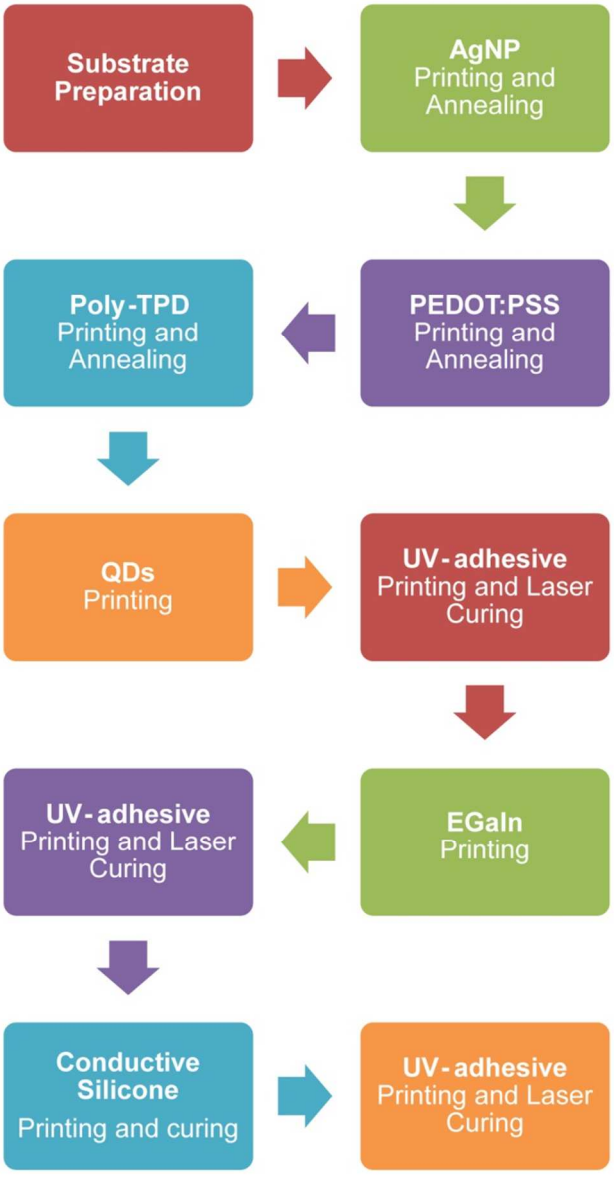

Figure S3. Process flow diagram for the 3D Printing of QD-LEDs.

Quantum Dot Ink Formulation

CdSe/ZnS QDs (Ocean NanoTech, San Diego, CA) was dissolved in toluene (Sigma Aldrich, St. Louis, MO) to 10 mg/ml. Dichlorobenzene (Sigma Aldrich, St. Louis, MO) and toluene were then added to dilute the concentration to 3 mg/ml with a volume fraction of 0-50% dichlorobenzene. A 25 mm × 25 mm indium tin oxide (ITO) coated glass slide (Sigma Aldrich,

St. Louis, MO) was cleaned with water, acetone and isopropanol for 15 minutes each. The ITO was then dried with nitrogen and heated to 150 ºC for 15 minutes. A 0.8 wt% PEDOT:PSS (Sigma Aldrich, St. Louis, MO) solution was then spin coated and heated at 150 ºC with a hotplate for 15 minutes. A 1.5 wt% poly-TPD (American Dye Source, Quebec, Canada) solution was then spin coated and heated at 110 ºC for 30 minutes. 0.5 µL of prepared QD solution was then dispensed with an auto micropipette as shown in the schematic of Fig. S4. The experiments were conducted under relative humidity of 22.5 ± 1 %, and temperature 23.5 ± 0.5 ºC. A hood was installed on top of the droplet to minimize disturbance from the environment while the mixture droplets evaporate. The QD droplet evaporation was visualized with the excitation from a 527 nm fluorescent lamp. The emission was filtered with a 540 nm filter and the fluorescent signal was recorded using a CCD camera. The lamp power was kept constant throughout the experiment, so that the intensity captured correlated with the deposition concentrations of the QDs of different droplets. The film heights were measured with a surface profiler (KLA-Tencor/P-15).

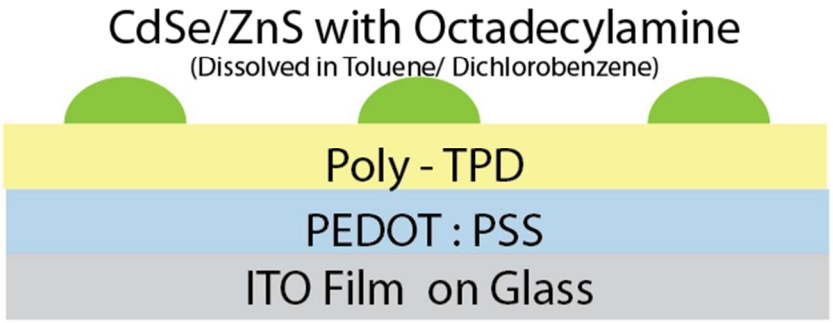

Figure S4. Schematic of experiments performed to understand the QD solvent-co-solvent formulation. Here, PEDOT:PSS and poly-TPD were spin coated on a cleaned ITO film on glass.

Poly-TPD

In contrast to spin coating, in which a significantly higher concentration (1.5 wt%) is typically used as the starting solution, we found that a device with appropriate diode characteristics was obtained when the concentration was reduced 10-18 fold (0.0825-0.15 wt%) during direct ink 3D printing. Indeed, printing studies conducted at the higher spin-coating concentrations resulted in non-uniform films with bulk resistances that were too high (2.44×10^9 Ω at 10 V). Comparable studies carried out at significantly diluted concentrations of poly-TPD (0.015 wt%) yielded unstable device performances due to the discontinuous surface of the poly-TPD layer .Poly-TPD (American Dye Source, Quebec, Canada) was dissolved in chlorobenzene (Fisher Scientific, Pittsburgh, PA) and dispensed on top of printed PEDOT:PSS. Also note that the formulation for the other layers was fixed in this particular QD-LED fabrication study to isolate the effect of the poly-TPD concentration on the resulting electrical performance.

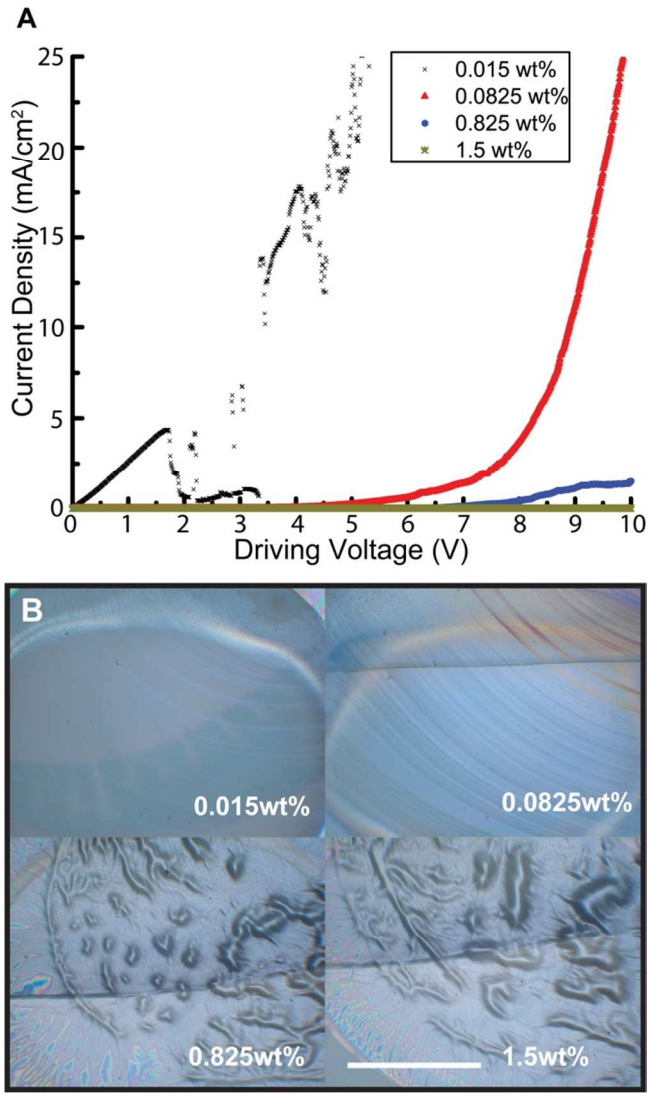

Figure S5. Poly-TPD concentration formulation and electrical performance of QD-LEDs. **(A)** Comparison of current density-voltage characteristics from devices made with different concentrations of poly-TPD. **(B)** Microscope images show film non-uniformity where the concentration was too high. The scale bar is 500 µm.

Synthesis of AgNPs

Polyacrylic acid-capped AgNPs were synthesized by modifying a previously published synthesis method.[1] Specifically, the following processing parameters have been modified due to the equipment availability. The particles were precipitated via centrifugation at 7,830 rpm for 1 hour (Eppendorf, Hauppauge, NY) and were homogenized at a speed of 100 rpm for 10 min

using an automatic solder paste mixing machine (Japan Unix Co, Akasaka, Japan). Conductive traces as small as 5 μm width were printed with the 3D printer. The morphology of the printed AgNP was characterized by scanning electron microscopy (Quanta 200 FEG Environmental-SEM), as shown in Figs. S6A and S6B. The silver precipitate was characterized with a transmission electron microscope (Philips CM100) (TEM, Fig. S6C). The particle sizes were measured from the TEM image and found to have an average diameter of 8.2 ± 5.0 nm. The printed AgNP had a resistivity of 10 Ω/cm after an hour of heating at 200 ºC.

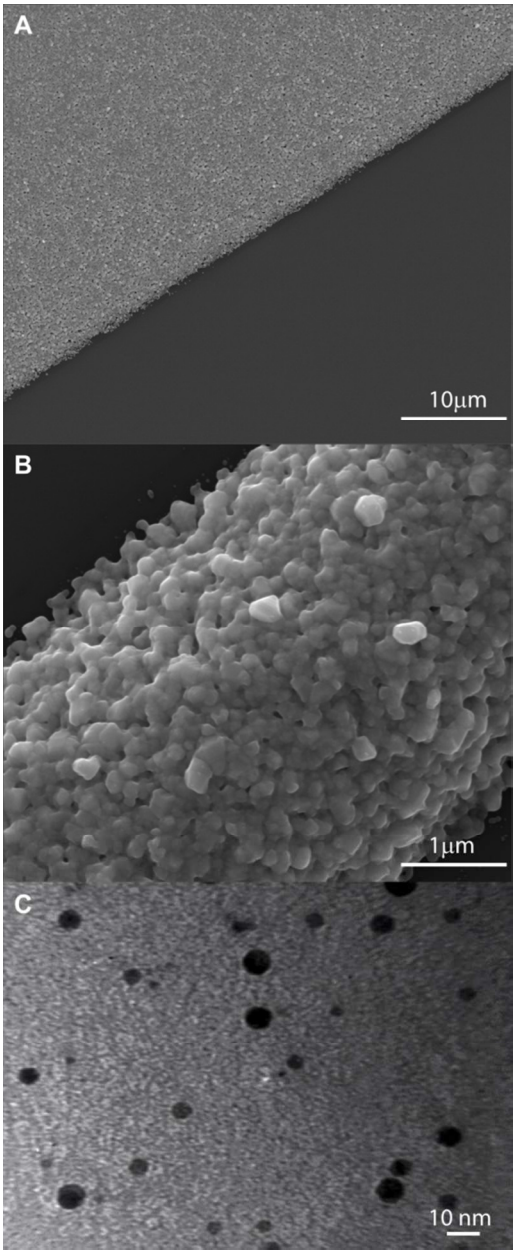

Figure S6. Characterization of synthesized AgNPs. **(A, B)** SEM images of synthesized AgNPs at different resolutions. **(C)** TEM images of synthesized AgNPs.

QD-LEDs Fabricated with AgNP as Cathode

This experiment was first conducted by 3D printing the synthesized AgNPs on a spin-coated device, where the spin-coated layers are similar to a previously published all-solution processed fabrication method.[2] Unlike the case for the EGaIn cathode, we found that AgNPs

require an additional electron transport layer to achieve electroluminescence. A 5 mg/ml solution of ZnO nanoparticles (Sigma Aldrich, St. Louis, MO) was printed as shown in Fig. S6A and then heated with a hotplate at 150 ºC for 30 minutes. The printed silver had a thickness of 80 μm, which was controlled by a combination of nozzle size (108 μm), printing speed (0.5 mm/s), gap height from the substrate (80 μm) and applied pressure. The ability to control the gap distance with a 3D printer is a critical factor in controlling the printing quality. If the gap is too small, excessive material would be squeezed out which would affect the planar resolution and annealing time; in contrast, when the gap is too large, the extruded material would not be continuously drawn to the substrate. In addition, it was found that careful control of both the annealing condition and printing pattern are important in achieving sintering of the AgNPs without damaging the underlying layer. A slow temperature ramping rate (10 ºC/min) and a spiral design were found to be necessary to provide a sufficient surface-area-to-volume ratio for removal of the solvent (water, ethylene glycol and polyacrylic acid) at a rate that causes insignificant damage to the underlying film. With a slow ramping rate and spiral design, a conductive cathode was formed. Fig. S7B shows the electroluminescence of the resulting QD-LED.

Once the parameter for cathode printing and sintering had been determined, we optimized the printing condition for poly-TPD and PEDOT:PSS with a similar approach as described previously. As shown in Fig. S7C, a fully printed design consists of a printed AgNP cathode and anode. Fig. S7C shows that the fully printed QD-LED achieves a luminance of 11 cd/m^2 at 13 V. The performance with the AgNP-based cathode was unsatisfactory by comparison with the EGaIn cathode for the following reasons. First, the printing of silver requires heating of 200 ºC for a minimum of 1 hour for its sintering process, which damages the underlying layers when it

is printed as a cathode under ambient conditions. Second, although bulk silver has a work function of -4.3 eV, AgNPs have large surface-to-volume ratios which allows them to be easily oxidized to silver oxide, which has a work function of -5.0 eV.[3]

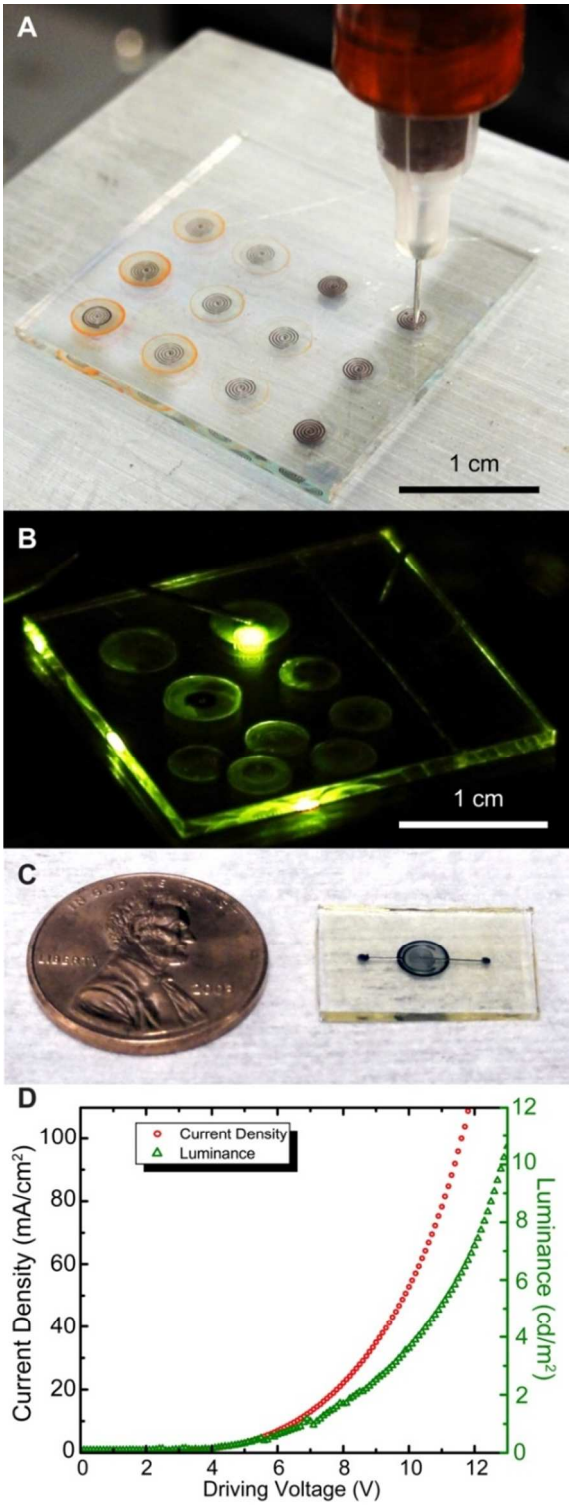

Figure S7. Fully printed QD-LED with AgNP cathode. **(A)** Image shows the printing of a spiral AgNP cathode. **(B)** Electroluminescence of QD-LED where ZnO and cathode were printed. **(C)** 3D printed QD-LED with AgNP cathode. **(D)** Current density and luminance of QD-LED from 0 to 12 V.

Printed QD-LEDs on Tape

Polyimide tape (McMaster-Carr, Robbinville, NJ) was attached to a glass slide. Commercially available AgNP dispersed in tetradecane (Sigma Aldrich, St. Louis, MO) was printed into a circular conductive ring (32 ga nozzle, 100 μm gap, 5 mm/s). The tape and conductive ring were then heated to 200 ºC for an hour to achieve a resistivity of 2.7 μΩ·cm. The subsequent layer of QD-LED was then printed as described earlier, with modification of the solvent-co-solvent ratio and QD concentrations. The QD-LED on the polyimide tape was then peeled slowly from the glass slide and reattached to different substrates, as demonstrated in Fig. S8. Figs. S8B to D were captured from the same printed QD-LED device that was transferred to different substrates, demonstrating the robust functionality of the 3D printed QD-LED despite undergoing repeated detachment and re-attachment.

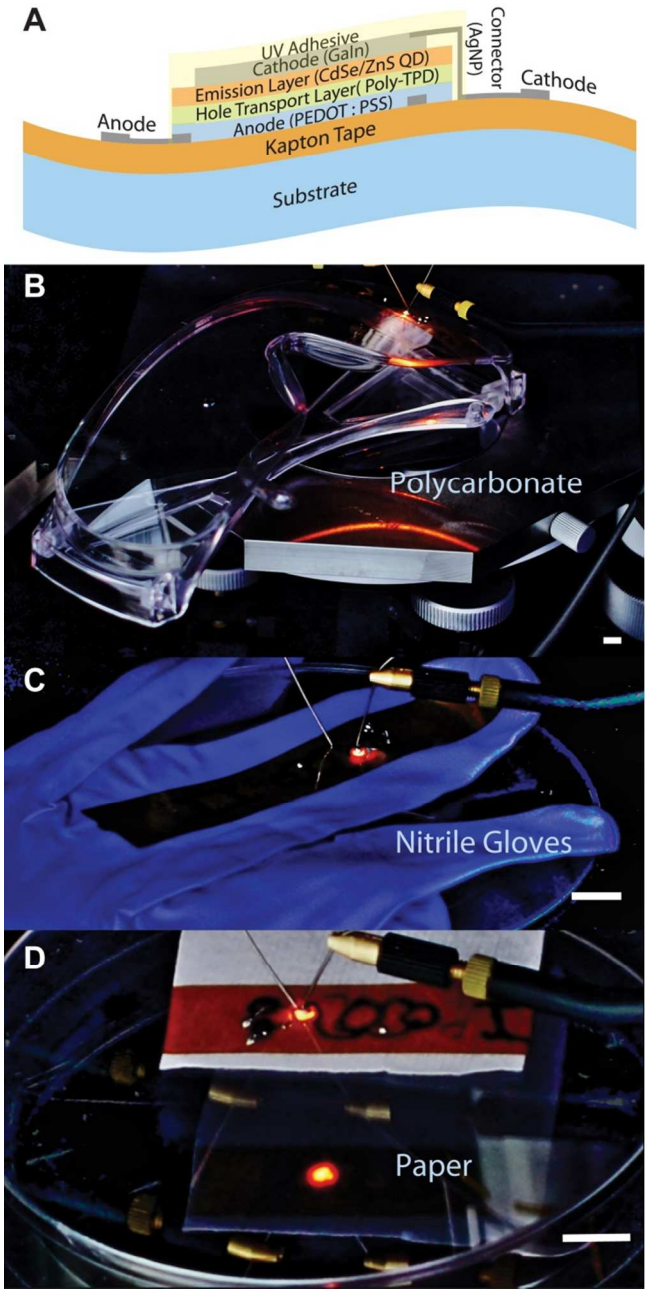

Figure S8. 3D printed QD-LED on a polyimide tape. **(A)** Schematic of printed QD-LED on polyimide tape. Photographs showing electroluminescence from an orange-red QD-LED on **(B)** a polycarbonate safety goggle, **(C)** nitrile gloves, and **(D)** paper. Scale bars are 1 cm.

Adhesion Layer for Fully Printed QD-LEDs

The suitability of five different printable transparent polymers as QD-LED substrates was assessed. As shown in Fig. S9, the contact angle of a PEDOT:PSS ink on (A) Novacentrix, PRO-001 UV, (B) polyvinyl alcohol (PVA), (C) polydimethylsiloxane (PDMS) (D) Norland Products Inc, UVS 91, (E) bifunctional acrylate monomers with photoinitiator (polyacrylate), and (F) glass, were investigated. PRO-001 UV consists of a blend of acrylate monomers and oligomers. UVS 91 consisted of mercapto-esters and tetrahydrofurfuryl methacrylate. The polyacrylate substrate consisted of ethoxylated bisphenol a-dimethacrylate bifunctional monomers and 1 wt% 2,2-dimethoxy-2-phenylacetophenone photoinitiator. The contact angle represents the solid-liquid adhesion energy per unit area. It was found the PRO-001 UV acrylate adhesive with a contact angle of 16 ± 4º exhibited good adhesion with PEDOT:PSS. Fig. S10 shows optical microscopy images of the annealed film. It was found that the PEDOT:PSS film was conductive on PRO-001 UV adhesive without sacrificing significant transparency. On the contrary, PEDOT:PSS does not adhere on hydrophobic substrates such as PDMS, and is non-conductive on substrates such as PVA. Based on these observations, the acrylate-based UV adhesive, PRO-001 UV was selected as a printable transparent substrate for subsequent experiments.

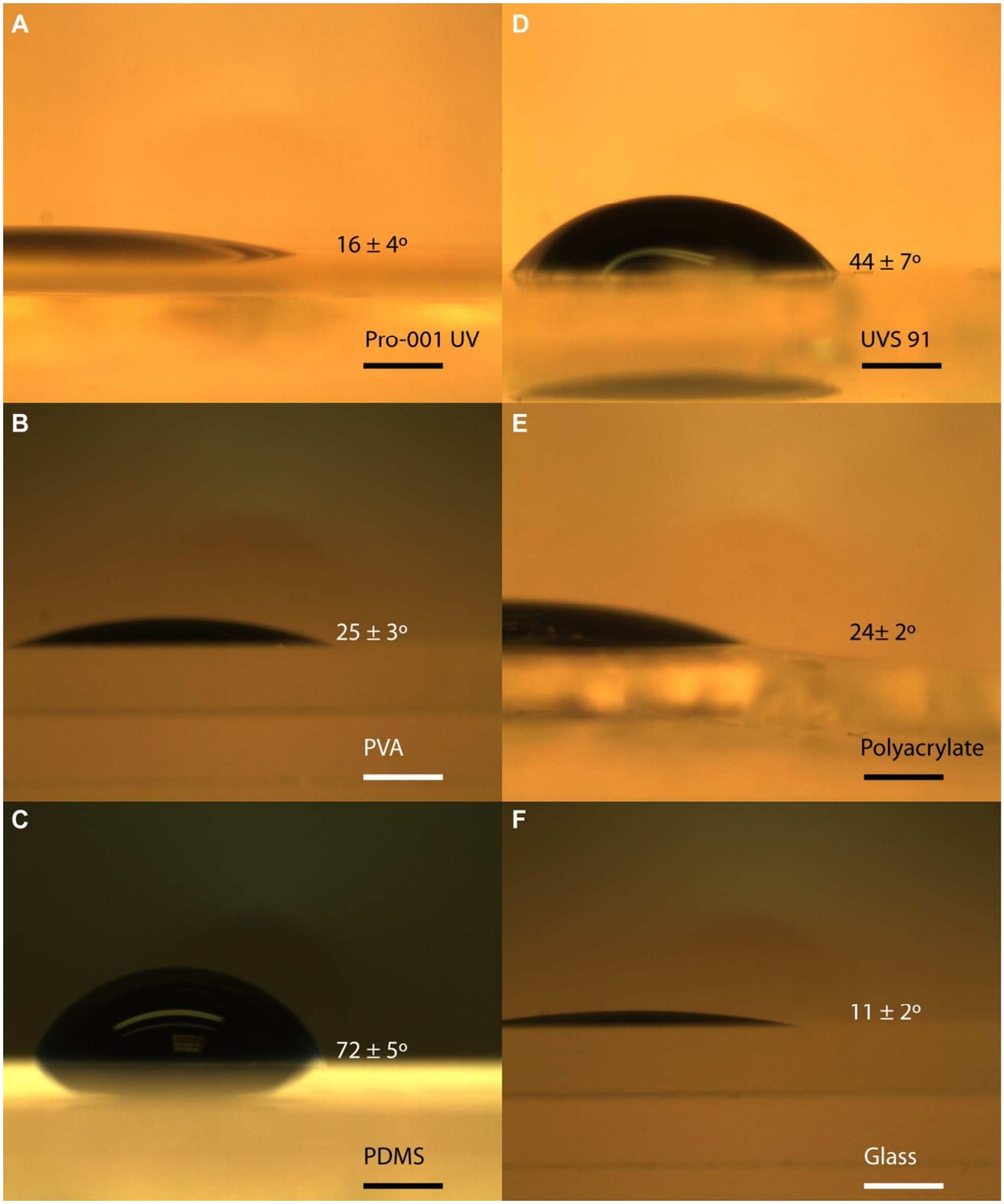

Figure S9. Contact angles of PEDOT:PSS ink on **(A)** PRO-001 UV, **(B)** polyvinyl alcohol (PVA) , **(C)** polydimethylsiloxane (PDMS), **(D)** UVS 91, **(E)** bifunctional acrylate monomers with photoinitiator (polyacrylate), and **(F)** glass. Scale bars are 1 mm.

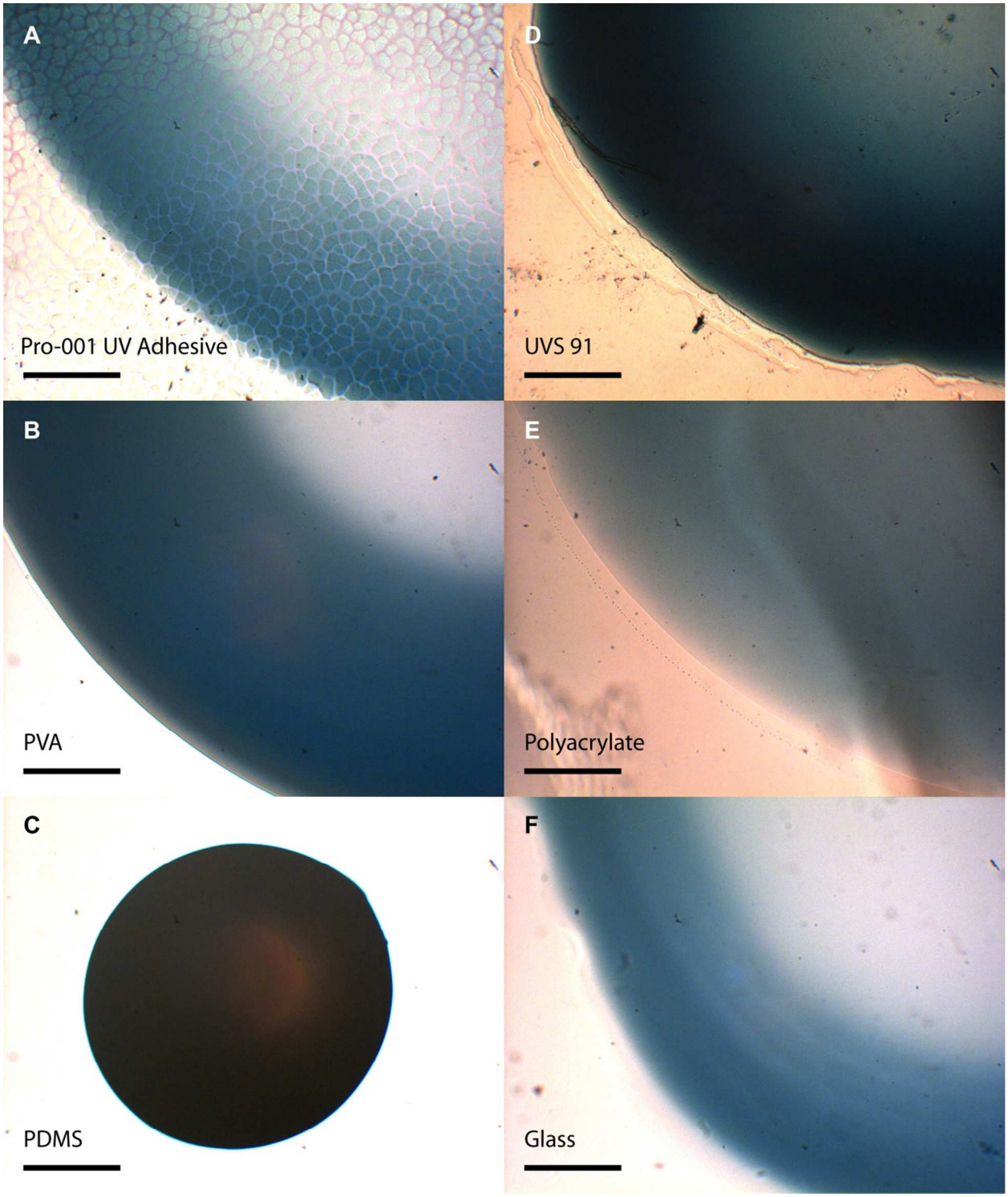

Figure S10. Annealed PEDOT:PSS ink on **(A)** PRO-001 UV, **(B)** polyvinyl alcohol (PVA), **(C)** polydimethylsiloxane (PDMS), **(D)** UVS 91, **(E)** bifunctional acrylate monomers with photoinitiator (polyacrylate), and **(F)** glass. Scale bars are 250 μm.

3D Structured Light Scanning of a Contact Lens

A hard contact lens (Winchester Optical Company, Elmira, NY) was imaged using a commercially available 3D structured-light scanner (SLS-1, David Visions, Germany) which resulted in geometrically faithful computer models of the contact lens surface, here representing the target curvilinear surface for conformal printing of QD-LEDs. Prior to scanning, a thin layer of contrast agent was applied to the lens to increase the density of data acquired per scan. The lens was then mounted at the center of a motorized rotational stage (Thorlabs, Newton, NJ). The scanner was calibrated and focused following vendor-provided protocols. Raw scan data was acquired without the use of scanning software-associated smoothing or filtering algorithms and was saved in wavefront OBJ data format. A total of eight scans of the lens were obtained at different rotational positions of the stage, ranging from 0 to 360 degrees in 45 degree intervals. The individual wavefront files were subsequently aligned and assembled using a mesh editing software (MeshLab) which resulted in a 3D mesh reconstruction of the contact lens. Briefly, alignment and assembly were carried out by point-based gluing alignment of the individual scans using ca. six identification points per scan. The data was then converted to a single 3D mesh by flattening visible layers, filling holes, and reconstructing a global surface.

The scanned model was then imported to Solidworks Premium 2014 with a ScanTo3D feature before the QD-LED CAD model was conformed to the surface of the model. A layer of UV adhesive (Novacentrix, Austin, TX) was then printed on the scanned hard contact lens as an adhesion layer. The adhesion layer was then cured with a handheld UV-lamp (285 nm) for an hour. The QD-LED was then printed, in which a concentration of 3 mg/ml solution of orange-red QDs (Ocean NanoTech, San Diego, CA) and 50% dichlorobenzene was used to achieve electroluminescence on the acrylate-based adhesive. To heat the layers without damaging the

substrate, the device was heated near the top layers via inversion, with a 1 mm air gap between the surface of the contact lens and the hot plate. The heating time was extended until the AgNP was sintered. The substrate was observed periodically and the gap was adjusted to prevent charring. For other layers, the hot plate temperature of the inverted configuration was increased until the temperature of the surface reached the prescribed surface temperature.

3D Printing of 2 × 2 × 2 QD-LED Array

The process flow of the printing is described in Fig. S11. A 3D CAD model, including the substrate and QD-LED array, were designed and rendered using Solidworks Premium 2014 (Dassault Systèmes, Vélizy-Villacoublay Cedex, France), then sent to the 3D printer for printing. Contact pads and connectors were printed on a glass substrate with synthesized AgNPs (33 ga, 80 μm gap, 50 psi pressure, 0.5 mm/s translation speed). A room temperature vulcanized silicone sealant (Loctitie, Rocky Hill, CT) was printed as the structural material. For silicone printing, tapered nozzle sizes ranged from 20 ga to 25 ga (610 μm to 250 μm) and the parameters were tailored based on the feature size, resolution and print speed. The print gap was maintained at 80% of the nozzle inner diameter, and the syringe barrel pressure ranged from 20-50 psi, depending on the translation speed. Prior to the printing of QD-LEDs on the printed silicone substrate, the UV adhesive previously identified (Novacentrix, Austin, TX) was printed and cured with a UV laser (405 nm) and a handheld UV lamp (285 nm). Multicolor QD-LEDs were then printed using the procedures described previously. To heat the layers without damaging the substrate, the device was inverted and heated near the top layers, with a ~1 mm air gap between the surface of the contact lens and the hot plate. The heating time was extended until the printed AgNPs were sintered. The substrate was observed periodically and the gap was adjusted to prevent charring. For other layers, the hot plate temperature of the inverted configuration was

increased until the temperature of the surface reached the prescribed surface temperature. As shown in Fig. S11, UV adhesive was printed to encapsulate the QD-LEDs before RTV silicone was printed as a structural material. Conductive silicone was printed as vertical interconnects, along with RTV silicone to connect the exposed EGaIn to the contact pads, and to connect the anode and cathode of the different layers.

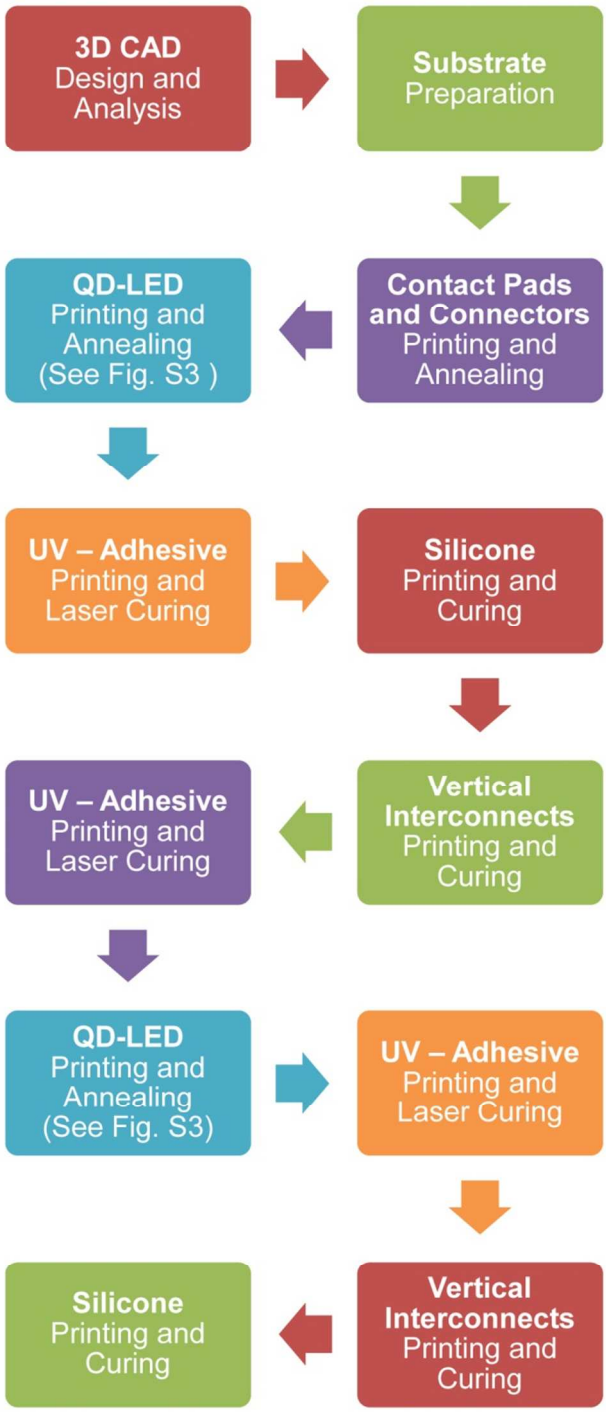

Figure S11. Process flow diagram for the 3D Printing of QD-LED arrays.

Movies

Movie 1. Video clip showing the evaporation of a dispensed droplet of QDs dissolved in pure toluene. The video has been sped up 49×.

Movie 2. Video clip showing the evaporation of a dispensed droplet of QDs dissolved in 80% toluene and 20% dichlorobenzene. The video has been sped up 24×.

Movie 3. Video clip showing the evaporation of a dispensed droplet of QDs dissolved in 50% toluene and 50% dichlorobenzene. The video has been sped up 54×.

REFERENCES

(1) Ahn, B. Y.; Duoss, E. B.; Motala, M. J.; Guo, X. Y.; Park, S. I.; Xiong, Y. J.; Yoon, J.; Nuzzo, R. G.; Rogers, J. A.; Lewis, J. A. *Science* **2009,** *323*, 1590-1593.
(2) Fuller, S. B.; Wilhelm, E. J.; Jacobson, J. M. *J. Microelectromech. Syst.* **2002,** *11*, 54-60.
(3) Girotto, C.; Rand, B. P.; Steudel, S.; Genoe, J.; Heremans, P. *Org. Electron.* **2009,** *10*, 735-740.